Concentration and energy fluctuations in a critical polymer mixture

M. Müller and N. B. Wilding
Institut für Physik, Johannes Gutenberg Universität, Staudinger Weg 7, D-55099 Mainz, Germany
(Received 20 May 1994; revised manuscript received 7 November 1994)

A semi-grand-canonical Monte Carlo algorithm is employed in conjunction with the bond-fluctuation model to investigate the critical properties of an asymmetric binary (AB) polymer mixture. By applying the equal peak-weight criterion to the concentration distribution, the coexistence curve separating the A-rich and B-rich phases is identified as a function of temperature and chemical potential. To locate the critical point of the model, the cumulant intersection method is used. The accuracy of this approach for determining the critical parameters of fluids is assessed. Attention is then focused on the joint distribution function of the critical concentration and energy, which is analyzed using a mixed-field finite-size-scaling theory that takes due account of the lack of symmetry between the coexisting phases. The essential Ising character of the binary polymer critical point is confirmed by mapping the critical scaling operator distributions onto independently known forms appropriate to the three-dimensional Ising universality class. In the process, estimates are obtained for the field mixing parameters of the model which are compared both with those yielded by a previous method and with the predictions of a mean-field calculation.

PACS number(s): 64.70.Ja, 05.70.Jk

I. INTRODUCTION

The critical point of binary liquid and binary polymer mixtures has been a subject of abiding interest to experimentalists and theorists alike for many years. It is now well established that the critical point properties of binary liquid mixtures fall into the Ising universality class (the default for systems with short ranged interactions and a scalar order parameter) [1]. Recent experimental studies also suggest that the same is true for polymer mixtures [2–11]. However, since Ising-like critical behavior is only apparent when the correlation length far exceeds the polymer radius of gyration $\xi \gg \langle R_g \rangle$, the Ising regime in polymer mixtures is confined (for all but the shortest chain lengths) to a very narrow temperature range near the critical point. Outside this range, a crossover to mean-field type behavior is seen. The extent of the Ising region is predicted to narrow with increasing molecular weight in a manner governed by the Ginsburg criterion [12], disappearing entirely in the limit of infinite molecular weight. Although experimental studies of mixtures with differing molecular weights appear to confirm qualitatively this behavior [5], there are severe problems in understanding the scaling of the so-called "Ginsburg number" (which marks the center of the crossover region and is empirically extracted from the experimental data [13]) with molecular weight.

Computer simulation potentially offers an additional source of physical insight into polymer critical behavior, complementing that available from theory and experiment. Unfortunately, simulations of binary polymer mixtures are considerably more exacting in computational terms than those of simple liquid or magnetic systems. The difficulties stem from the problems of dealing with the extended physical structure of polymers. In conventional canonical simulations, this gives rise to extremely slow polymer diffusion rates, manifested in protracted correlation times [14,15]. Moreover, the canonical ensemble does not easily permit a satisfactory treatment of concentration fluctuations, which are an essential feature of the near-critical region in the polymer mixture. In this latter regard, semi-grand-canonical ensemble (SGCE) Monte Carlo schemes are potentially more attractive than their canonical counterparts. In SGCE schemes, one attempts to exchange a polymer of species A for one of species B or vice versa, thereby permitting the concentration of the two species to fluctuate. Owing, however, to excluded-volume restrictions, the acceptance rate for such exchanges is, in general, prohibitively small, except in the restricted case of symmetric polymer mixtures, where the molecular weights of the two coexisting species are identical ($N_A = N_B$). All previous simulation work has, therefore, focused on these symmetric systems, mapping the phase diagram as a function of chain length and confirming the Ising character of the critical point [16–18]. Tentative evidence for a crossover from Ising to mean-field behavior away from the critical point was also obtained [19]. Hitherto, however, no simulation studies of asymmetric polymer mixtures ($N_A \neq N_B$) have been reported.

Recently one of us developed a SGCE Monte Carlo method that ameliorates somewhat the computational difficulties of dealing with asymmetric polymer mixtures [20]. The method, which is described briefly in Sec. III A, permits the study of mixtures of polymer species of molecular weight N_A and $N_B = kN_A$, with $k = 2,3,4,\ldots$. In this paper, we shall employ this method to investigate the critical behavior of such an asymmetric polymer mixture. In particular, we shall focus on those aspects of the critical behavior of asymmetric mixtures that differ from those of symmetric mixtures. These differences are rooted in the so-called "field mixing" phenomenon, which

manifests the basic lack of energetic (Ising) symmetry between the coexisting phases of all realistic fluid systems. Although it is expected to have no bearing on the universal properties of fluids, field mixing does engender certain nonuniversal effects in near-critical fluids. The most celebrated of these is a weak energylike critical singularity in the coexistence diameter [21,22], the existence of which constitutes a failure for the "law of rectilinear diameter." As we shall demonstrate, however, field mixing has a far more legible signature in the interplay of the near-critical energy and concentration fluctuations, which are directly accessible to computer simulation.

In computer simulation of critical phenomena, finite-size-scaling (FSS) techniques are of great use in allowing one to extract asymptotic data from simulations of finite size [23]. One particularly useful tool in this context is the order parameter distribution function [24–26]. Simulation studies of magnetic systems such as the Ising [25] and ϕ^4 models [27], demonstrate that the critical point form of the order parameter distribution function constitutes a useful hallmark of a universality class. Recently, however, FSS techniques have been extended to fluids by incorporating field mixing effects [28,29]. The resulting mixed-field FSS theory has been successfully deployed in Monte Carlo studies of critical phenomena in the two-dimensional (2D) Lennard-Jones fluid [29] and the 2D asymmetric lattice gas model [30].

The present work extends this program of field mixing studies to 3D complex fluids with an investigation of an asymmetric polymer mixture. The principal features of our study are as follows. We begin by studying the order parameter (concentration) distribution as a function of temperature and chemical potential. The measured distribution is used in conjunction with the equal peak-weight criterion to obtain the coexistence curve of the model. Owing to the presence of field mixing contributions to the concentration distribution, the equal weight criterion is found to break down near the fluid critical point. Its use to locate the coexistence curve and critical concentration, therefore, results in errors, the magnitude of which we gauge using scaling arguments. The field mixing component of the critical concentration distribution is then isolated and used to obtain estimates for the field mixing parameters of the model. These estimates are compared with the results of a mean-field calculation.

We then turn our attention to the finite-size-scaling behavior of the critical *scaling operator* distributions. This approach generalizes that of previous field mixing studies, which concentrated largely on the field mixing contribution to the order parameter distribution function. We show that for certain choices of the nonuniversal critical parameters—the critical temperature, chemical potential, and the two field mixing parameters—these operator distributions can be mapped into close correspondence with independently known univerasl forms representative of the Ising universality class. This data collapse serves two purposes. First, it acts as a powerful means for accurately determining the critical point and field mixing parameters of model fluid systems. Second, and more generally, it serves to clarify the *sense* of the universality linking the critical polymer mixture with the critical Ising magnet. We compare the ease and accuracy with which the critical parameters can be determined from the data collapse of the operator distributions, with that possible from studies of the order parameter distribution alone. It is argued that for critical fluids the study of the scaling operator distributions represent the natural extension of the order parameter distribution analysis developed for models of the Ising symmetry.

II. BACKGROUND

In this section, we review and extend the mixed-field finite-size-scaling theory, placing it within the context of the present study.

The system we consider comprises a mixture of two polymer species, which we denote A and B, having lengths N_A and N_B monomers, respectively. The configurational energy Φ (which we express in units of k_BT) resides in the intramolecular and intermolecular pairwise interactions between monomers of the polymer chains:

$$\Phi(\{\mathbf{r}\})=\sum_{i<j=1}^{\mathcal{N}} v(|\mathbf{r}_i-\mathbf{r}_j|) , \tag{2.1}$$

where $\mathcal{N}=n_AN_A+n_bN_B$ with n_A and n_B the number of A- and B-type polymers, respectively. $\mathcal{N}$ is, therefore, the total number of monomers (of either species), which in the present study is maintained strictly constant. The intermonomer potential v is assigned a square-well form

$$\begin{aligned} v(r)&=-\epsilon, \quad r\le r_m , \\ v(r)&=0, \quad r>r_m , \end{aligned} \tag{2.2}$$

where ϵ is the well depth and r_m denotes the maximum range of the potential. In accordance with previous studies of symmetric polymer mixtures [16,17], we assign $\epsilon\equiv\epsilon_{AA}=\epsilon_{BB}=-\epsilon_{AB}>0$.

The independent model parameters at our disposal are the chemical potential difference per monomer between the two species $\Delta\mu=\mu_A-\mu_B$, and the well depth ϵ (both in units of k_BT). These quantities serve to control the observables of interest, namely the energy density u and the monomer concentrations ϕ_A and ϕ_B. Since the overall monomer density $\phi_{\mathcal{N}}=\phi_A+\phi_B$ is fixed, however, it is sufficient to consider only one concentration variable ϕ, which we take as the concentration of A-type monomers:

$$\phi\equiv\phi_A=L^{-d}n_AN_A . \tag{2.3}$$

The dimensionless energy density is defined as

$$u=L^{-d}\epsilon^{-1}\Phi(\{\mathbf{r}\}) , \tag{2.4}$$

with $d=3$ in the simulations to be chronicled below.

The critical point of the model is located by critical values of the reduced chemical potential difference $\Delta\mu_c$ and reduced well depth ϵ_c. Deviations of ϵ and $\Delta\mu$ from their critical values control the sizes of the two relevant scaling fields that characterize the critical behavior. In the absence of the special symmetry prevailing in the Ising model, one finds that the relevant scaling fields

comprise (asymptotically) *linear combinations* of the well depth and chemical potential difference [21]

$$\tau=\epsilon_c-\epsilon+s(\Delta\mu-\Delta\mu_c),\quad h=\Delta\mu-\Delta\mu_c+r(\epsilon_c-\epsilon)\ , \tag{2.5}$$

where τ is the thermal scaling field and h is the ordering scaling field. The parameters s and r are system-specified quantities controlling the degree of field mixing. In particular, r is identifiable as the limiting critical gradient of the coexistence curve in the space of $\Delta\mu$ and ϵ. The role of s is somewhat less tangible; it controls the degree to which the chemical potential features in the thermal scaling field manifest in the widely observed critical singularity of the coexistence curve diameter of fluids [1,22,31].

Conjugate to the two relevant scaling fields are scaling operators $\mathcal{E}$ and $\mathcal{M}$, which comprise linear combinations of the concentration and energy density [28,29]:

$$\mathcal{M}=\frac{1}{1-sr}[\phi-su],\quad \mathcal{E}=\frac{1}{1-sr}[u-r\phi]\ . \tag{2.6}$$

The operator $\mathcal{M}$ (which is conjugate to the ordering field h) is termed the ordering operator, while $\mathcal{E}$ (conjugate to the thermal field) is termed the energylike operator. In the special case of models of the Ising symmetry, (for which $s=r=0$), $\mathcal{M}$ is simply the magnetization while $\mathcal{E}$ is the energy density.

Near criticality, and in the limit of large system size L, the probability distributions $p_L(\mathcal{M})$ and $p_L(\mathcal{E})$ of the operators $\mathcal{M}$ and $\mathcal{E}$ are expected to be describable by finite-size-scaling relations having the form [25,29]

$$p_L(\mathcal{M})\simeq a_{\mathcal{M}}^{-1}L^{d-\lambda_{\mathcal{M}}} \times\tilde{p}_{\mathcal{M}}(a_{\mathcal{M}}^{-1}L^{d-\lambda_{\mathcal{M}}}\delta\mathcal{M},a_{\mathcal{M}}L^{\lambda_{\mathcal{M}}}h,a_{\mathcal{E}}L^{\lambda_{\mathcal{E}}}\tau)\ , \tag{2.7a}$$

$$p_L(\mathcal{E})\simeq a_{\mathcal{E}}^{-1}L^{d-\lambda_{\mathcal{E}}}\tilde{p}_{\mathcal{E}}(a_{\mathcal{E}}^{-1}L^{d-\lambda_{\mathcal{E}}}\delta\mathcal{E},a_{\mathcal{M}}L^{\lambda_{\mathcal{M}}}h,a_{\mathcal{E}}L^{\lambda_{\mathcal{E}}}\tau)\ , \tag{2.7b}$$

where $\delta\mathcal{M}\equiv\mathcal{M}-\mathcal{M}_c$ and $\delta\mathcal{E}\equiv\mathcal{E}-\mathcal{E}_c$. The functions $\tilde{p}_{\mathcal{M}}$ and $\tilde{p}_{\mathcal{E}}$ are predicted to be *universal,* modulo the choice of boundary conditions and the system-specific scale-factors $a_{\mathcal{M}}$ and $a_{\mathcal{E}}$ of the two relevant fields, whose scaling indices are $\lambda_{\mathcal{M}}=d-\beta/\nu$ and $\lambda_{\mathcal{E}}=1/\nu$, respectively. Precisely at criticality ($h=\tau=0$), Eqs. (2.7a) and (2.7b) imply

$$p_L(\mathcal{M})\simeq a_{\mathcal{M}}^{-1}L^{\beta/\nu}\tilde{p}^{\,*}_{\mathcal{M}}(a_{\mathcal{M}}^{-1}L^{\beta/\nu}\delta\mathcal{M})\ , \tag{2.8a}$$

$$p_L(\mathcal{E})\simeq a_{\mathcal{E}}^{-1}L^{(1-\alpha)/\nu}\tilde{p}^{\,*}_{\mathcal{E}}(a_{\mathcal{E}}^{-1}L^{(1-\alpha)/\nu}\delta\mathcal{E})\ , \tag{2.8b}$$

where

$$\tilde{p}^{\,*}_{\mathcal{M}}(x)\equiv\tilde{p}_{\mathcal{M}}(x,y=0,z=0)\ ,\qquad \tilde{p}^{\,*}_{\mathcal{E}}(x)\equiv\tilde{p}_{\mathcal{E}}(x,y=0,z=0) \tag{2.9}$$

are functions describing the universal and statistically scale-invariant fluctuation spectra of the scaling operators, characteristic of the critical point.

The claim that the binary polymer critical point belongs to the Ising universality class is expressed in its fullest form by the requirement that the critical distribution of the fluid scaling operators $p_L(\mathcal{M})$ and $p_L(\mathcal{E})$ match quantitatively their respective counterparts—the magnetization and energy distributions—in the canonical ensemble of the critical Ising magnet. As we shall demonstrate, these mappings also permit a straightforward and accurate determination of the values of the field mixing parameters s and r of the model.

An alternative route to obtaining estimates of the field mixing parameters is via the field mixing correction to the order parameter (i.e., concentration) distribution $p_L(\phi)$. At criticality, this distribution takes the form [29,30]

$$p_L(\phi)\simeq a_{\mathcal{M}}^{-1}L^{\beta/\nu}\left[\tilde{p}^{\,*}_{\mathcal{M}}(x)-sa_{\mathcal{E}}a_{\mathcal{M}}^{-1}L^{-(1-\alpha-\beta)/\nu}\frac{\partial}{\partial x}\times(\tilde{p}^{\,*}_{\mathcal{M}}(x)\tilde{\omega}^{\,*}(x))+O(s^2)\right]_{x=a_{\mathcal{M}}^{-1}L^{\beta/\nu}[\phi-\phi_c]}\ , \tag{2.10}$$

where

$$\tilde{\omega}^{\,*}(x)=a_{\mathcal{E}}^{-1}L^{d-1/\nu}[\langle u(\phi)\rangle-u_c-r(\phi-\phi_c)]+O(s)\ , \tag{2.11}$$

which we term the energy function, is a universal function characterizing the critical energylike operator. Equation (2.10) states that to leading order in the field mixing parameter s, the order parameter distribution is a sum of two distinct universal components. The first of these, $\tilde{p}^{\,*}_{\mathcal{M}}(x)$, is simply the universal ordering operator distribution featuring in Eq. (2.8a). The second, $\partial/\partial x(\tilde{p}^{\,*}_{\mathcal{M}}(x)\tilde{\omega}^{\,*}(x))$, is a function characterizing the mixing of the critical energylike operator into the order parameter distribution. This field mixing term is down on the first term by a factor $L^{-(1-\alpha-\beta)/\nu}$ and, therefore, represents a *correction* to the large L limiting behavior. Given further the symmetries of $\tilde{\omega}(x)$ and $\tilde{p}^{\,*}_{\mathcal{M}}(x)$, both of which are even (symmetric) in the scaling variable x [29], the field mixing correction is the leading antisymmetric contribution to the concentration distribution. Accordingly, it can be isolated from measurements of the critical concentration distribution simply by antisymmetrizing around $\phi_c=\langle\phi\rangle_c$. The values of s and r are then obtainable by matching the measured critical function $-s\partial/\partial\phi\{p_L(\phi)[\langle u(\phi)\rangle-u_c-r(\phi-\phi_c)]\}$ to the measured antisymmetric component of the critical concentration distribution [30]. In the simulations described below, we shall compare the values of s and r obtained by this method with those obtained by matching the fluid operator distributions to their Ising equivalent forms.

Finally, in this section, we turn to a consideration of the finite-size-scaling behavior of the energy distribution function. In contrast to the situation for the order parameter distribution described above, it transpires that field mixing radically alters the *limiting* form of the critical energy density distribution. To substantiate this claim, we reexpress u in terms of the scaling operators. Appealing to Eq. (2.6), one finds

$$u=\mathcal{E}+r\mathcal{M}\ , \tag{2.12}$$

so that the critical energy density distribution is

$$p_L(u)=p_L(\mathcal{E}+r\mathcal{M}) . \quad (2.13)$$

Now the structure of the scaling forms (2.8a) and (2.8b) show that the typical size of the fluctuations in the energylike operator will vary with system size like $\delta\mathcal{E}\sim L^{-(1-\alpha)/\nu}$, while the typical size of the fluctuations in the ordering operator vary like $\delta\mathcal{M}\sim L^{-\beta/\nu}$. Given that in general $\alpha<\beta$, it follows that asymptotically, the contribution of $\mathcal{E}$ to the argument on the right hand side of Eq. (2.13) can be neglected, so that

$$p_L(u)\simeq p_L(r\mathcal{M})\simeq a_{\mathcal{M}}^{-1} r L^{\beta/\nu}\tilde{p}^{*}_{\mathcal{M}}(a_{\mathcal{M}}^{-1} r L^{\beta/\nu}\delta\mathcal{M}) . \quad (2.14)$$

We conclude then that for sufficiently large L, the distribution of the fluid critical energy density has the same functional form as the distribution of the critical ordering operator $\tilde{p}^{*}_{\mathcal{M}}$. Given further that $\tilde{p}^{*}_{\mathcal{M}}$ possesses a *symmetric double-peaked* form, while the critical energy distribution in the Ising model $p_L(u)=\tilde{p}^{*}_{\mathcal{E}}$ possesses an *asymmetric single-peaked* form, the profound influence of field mixing on the critical energy distribution of fluids should be apparent.

III. MONTE CARLO STUDIES

A. Algorithmic and computational aspects

The polymer model studied in this paper is the bond-fluctuation model (BFM). The BFM is a coarse-grained lattice-based model that combines computational tractability with the important qualitative features of real polymers: monomer excluded volume, monomer connectivity, and short range interactions. Within the framework of the model, each monomer occupies a whole unit cell of a 3D periodic simple cubic lattice. Neighboring monomers along the polymer chains are connected via one of 108 possible bond vectors. These bond vectors provide for a total of 5 different bond lengths and 87 different bond angles. Thermal interactions are catered for by a short range intermonomer potential. Further details concerning the model can be found in Ref. [32].

The system we have studied comprises two polymer species A and B having chain lengths N_A and N_B with $N_B=kN_A$. The SGCE scheme whereby polymers of type A are transformed into polymers of type B (or vice versa) is described in the Appendix and in Ref. [20], but in general terms operates as follows. Using a Metropolis algorithm, an A-type polymer is formed simply by cutting a B-type polymer into k equal segments. Conversely, a B-type polymer is manufactured by connecting together the ends of k A-type polymers. This latter operation is, of course, subject to the condition that the connected ends satisfy the bond restrictions of the BFM. Consequently, it represents the limiting factor for the efficiency of the method, since for large values of k and N_A, the probability that k polymer ends simultaneously satisfy the bond restrictions becomes prohibitively small. The acceptance rate for SGCE moves is also further reduced by factors necessary to ensure that detailed balance is satisfied. In view of this, we have chosen $k=3$, $N_A=10$ for the simulations described below, resulting in an acceptance rate for SGCE moves of approximately 14%.

In addition to the compositional fluctuations associated with SGCE moves, it is also necessary to relax the polymer configurations at constant composition. This is facilitated by monomer moves, which can be either of the local displacement form, or of the reptation ("slithering snake") variety [2]. These moves were employed in conjunction with SGCE moves, in the following ratios:

local displacement : reptation : semi-grand-canonical

$$=4:12:1 ,$$

the choice of which was found empirically to relax the configurational and compositional modes of the system on approximately equal time scales.

In the course of the simulations, a total of five system sizes were studied having linear extent $L=32$, 40, 50, 64, and 80. An overall monomer filling fraction of $8\phi_N=0.5$ was chosen, representative of a dense polymer melt [15]. Here the factor of 8 constitutes the monomeric volume, each monomer occupying eight lattice sites. The cutoff range of the intermonomeric square-well potential was set at $r_m=\sqrt{6}$ (in units of the lattice spacing), a choice which ensures that the first peak of the correlation function is encompassed within the range of the potential. The observables sampled in the simulations were the A-monomer concentration ϕ and the energy density u [cf., Eqs. (2.3) and (2.4)]. The joint distribution $p_L(\phi,u)$ of these quantities was accumulated in the form of a histogram, with successive samples being separated by 12.5 semi-grand-canonical sweeps in order to reduce correlations. The final histograms for the lattice sizes $L=40$ and 64 each comprised some 5×10^5 entries. Assistance in exploring the phase space of the model, was provided by means of the multihistogram reweighting technique [33,34]. This technique allows one to generate estimated histograms $p_L(\phi,u)$ for values of the control parameters ϵ and $\Delta\mu$ other than those at which the simulations were actually performed. Such extrapolations are generally very reliable in the neighborhood of the critical point, due to the large critical fluctuations [33].

B. The coexistence curve and critical limit

In general, for fluid systems, the coexistence curve is not known *a priori* and must, therefore, be identified empirically as a prelude to locating the critical point itself. One computational criterion that can be used to effect this identification is the so-called "equal weight criterion" for the order parameter (concentration) distribution function $p_L(\phi)=\int du p_L(\phi,u)$ [35]. Precisely on coexistence and for temperatures well below criticality, $p_L(\phi)$ will comprise two well-separated Gaussian peaks of equal weight, but unequal heights and widths. The centers of these peaks identify the concentrations of the coexisting A-rich and A-poor phases. For a given subcritical well depth ϵ, the coexistence value for the chemical potential difference $\Delta\mu_{cx}$ can, therefore, be obtained by adjusting $\Delta\mu$ until the concentration distribution satisfies the condition

$$\int_0^{\phi^*} p_L(\phi,\epsilon,\Delta\mu_{cx})d\phi = \int_{\phi^*}^{\phi_{\mathcal{N}}} p_L(\phi,\epsilon,\Delta\mu_{cx})d\phi \ , \tag{3.1}$$

where ϕ^* is a parameter defining the boundary between the two peaks.

Well below criticality, the value of $\Delta\mu_{cx}$ obtained from the equal weight criterion is insensitive to the choice of ϕ^*, provided it is taken to lie approximately midway between the peaks and well away from the tails. As criticality is approached, however, the tails of the two peaks progressively overlap making it impossible to unambiguously define a peak in the manner expressed by Eq. (3.1). For models of the Ising symmetry, for which the peaks are symmetric about the coexistence concentration ϕ_{cx}, the correct value of $\Delta\mu_{cx}$ can nevertheless be obtained by choosing $\phi^* = \langle\phi\rangle$ in Eq. (3.1). In near-critical fluids, however, the imposed equal weight rule forces a shift in the chemical potential away from its coexistence value in order to compensate for the presence of the field mixing component. Only in the limit as $L \to \infty$ (where the field mixing component dies away), will the critical order parameter distribution be symmetric allowing one to choose $\phi^* = \langle\phi\rangle$ and still obtain the correct coexistence chemical potential. Thus, for finite-size systems, use of the equal weight criterion is expected to lead to errors in the determination of $\Delta\mu_{cx}$ near the critical point. Although this error is much smaller than the uncertainty in the location of the critical point *along* the coexistence curve (see below), it can lead to significant errors in estimates of the critical concentration ϕ_c.

To quantify the error in ϕ_c, it is necessary to match the magnitude of the field mixing component of the concentration distribution $w(\delta p_L)$, to the magnitude of the peak-weight asymmetry $w'(\delta\mu)$ associated with small departures $\delta\mu = \Delta\mu - \Delta\mu_{cx}$ from coexistence

$$w(\delta p_L) = w'(\delta\mu) \ . \tag{3.2}$$

Now, from Eq. (2.10)

$$w(\delta p_L) \approx \int_{\phi^*}^{\phi_{\mathcal{N}}} d\phi \, \delta p_L(\phi) \sim L^{-(1-\alpha-\beta)/\nu} \ , \tag{3.3}$$

while

$$w'(\delta\mu) \approx \int_{\phi^*}^{\phi_{\mathcal{N}}} d\phi \frac{\partial p_L(\phi)}{\partial\Delta\mu}\delta\mu \propto L^{(\beta+\gamma)/\nu}\delta\mu \ . \tag{3.4}$$

It follows that the error in $\Delta\mu_{cx}$ varies with system size like

$$\delta\mu \propto L^{-(1-\alpha+\gamma)/\nu} \ . \tag{3.5}$$

Accordingly, the error in the critical concentration (obtained as the first moment of the concentration distribution) varies with system size like

$$\delta\phi_c = \chi(L)\delta\mu = L^{\gamma/\nu}\delta\mu \sim L^{-(1-\alpha)/\nu} \ . \tag{3.6}$$

Note also that an analogous treatment of the shift in the auxiliary variable ϕ^* leads to the same L dependence.

Measurements of the concentration distribution were performed in conjunction with the equal weight criterion, to locate the coexistence curve as a function of well depth and chemical potential. The results are shown in Fig. 1. Since in finite-size systems, the order parameter distribution exhibits a double-peaked structure even above the critical temperature, the data shown also represent the analytic continuation of the true coexistence curve that persists in finite-size systems [29]. To determine the position of the critical point on this line of pseudocoexistence, the cumulant intersection method was employed. The fourth-order cumulant ratio G_L is a dimensionless quantity that characterizes the form of a function. It is defined as

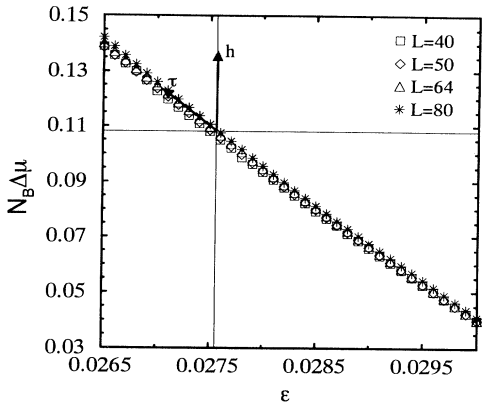

FIG. 1. The measured line of pseudo-phase-coexistence separating the A-rich and A-poor phases, for which the concentration distribution has two peaks of equal weight. The position of the critical point as determined using the cumulant intersection method (see also Fig. 2) is indicated, as are the measured directions of the two relevant scaling fields h and τ.

$$G_L = 1 - \frac{\langle m^4\rangle}{3\langle m^2\rangle^2} \ , \tag{3.7}$$

where m^2 and m^4 are the second and fourth moments, respectively, of the order parameter $m = \phi - \langle\phi\rangle$. To the extent that field mixing corrections can be neglected, the critical order parameter distribution function is expected to assume a universal scale invariant form. Accordingly, when plotted as a function of ϵ, the coexistence values of G_L for different system sizes are expected to intersect at the critical well depth ϵ_c [26]. This method is particularly attractive for locating the critical point in fluid systems because the even moments of the order parameter distribution are insensitive to the antisymmetric (odd) field mixing contribution. Figure 2 displays the results of performing this cumulant analysis. A well-defined intersection point occurs for a value $G_L = 0.47$, in accordance with previously published values for the 3D Ising universality class [36]. The corresponding estimates for the critical well depth and critical chemical potential are

$$\epsilon_c = 0.027\,56(15), \quad \Delta\mu_c = 0.003\,603(15) \ .$$

It is important in this context that a distinction be drawn between the errors on the location of the critical point, and the error with which the coexistence curve can be determined. The uncertainty in the position of the critical point *along* the coexistence curve, as determined from the cumulant intersection method is, in general,

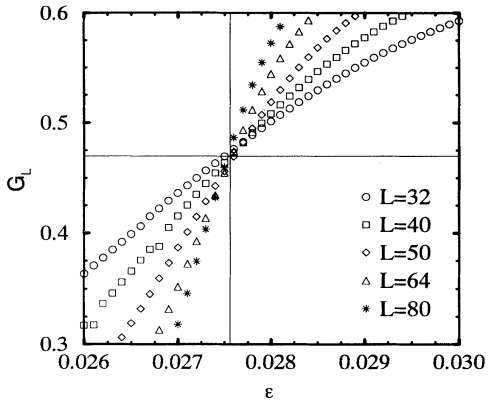

FIG. 2. The value of the fourth-order cumulant ratio $G_L = 1 - \langle m^4 \rangle / 3 \langle m^2 \rangle^2$ with $m = \phi - \phi_{cx}$, expressed as a function of system size L and well depth ϵ, along the line of pseudo-phase-coexistence. An intersection occurs for a value of $G_L = 0.47$ at $\epsilon_c = 0.027\,56(15)$, $\Delta\mu_c = 0.003\,603(15)$.

considerably greater than the uncertainty in the location of the coexistence curve itself. This is because the order parameter distribution function is much more sensitive to small deviations off coexistence (due to finite $\epsilon - \epsilon_{cx}$ or finite $\Delta\mu - \Delta\mu_{cx}$) than it is for deviations along the coexistence curve (ϵ and $\Delta\mu$ tuned together to maintain equal weights). In the present case, we find that the errors on $\Delta\mu_c$ and ϵ_c are approximately ten times those of the coexistence values ϵ_{cx} and $\Delta\mu_{cx}$ near the critical point.

The concentration distribution function at the assigned value ϵ_c and the corresponding value of $\Delta\mu_{cx}$, (determined according to the equal weight rule with $\phi^* = \langle \phi \rangle$), is shown in Fig. 3 for the $L = 40$ and $L = 64$ system sizes.

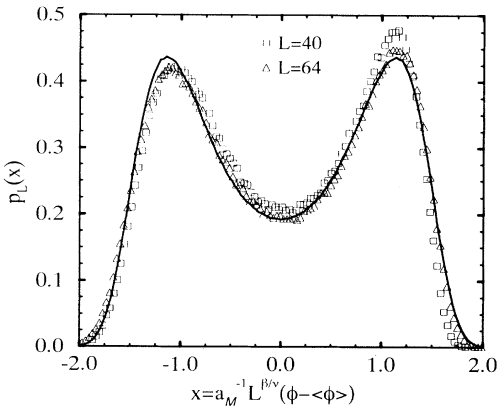

FIG. 3. The normalized concentration distribution for the $L = 40$ and $L = 64$ system sizes obtained using the equal weight criterion with $\phi^* = \langle \phi \rangle$, at the assigned value of the critical well depth $\epsilon = 0.027\,56(15)$. The data are expressed in terms of the scaling variable $x = a_{\mathcal{M}}^{-1} L^{\beta/\nu}(\phi - \phi_c)$, where the nonuniversal scale factor $a_{\mathcal{M}}^{-1}$ has been chosen so that distributions have unit variance. Also shown (solid) curve is the fixed point function $\tilde{p}^*_{\mathcal{M}}$ appropriate to the 3D Ising universality class. Statistical errors do not exceed the symbol sizes.

Also shown in the figure is the critical magnetization distribution function of the 3D Ising model obtained in a separate study [37]. Clearly the $L = 40$ and $L = 64$ data differ from one another and from the limiting Ising form. These discrepancies manifest both the pure antisymmetric field mixing component of the true (finite-size) critical concentration distribution, and small departures from coexistence associated with the inability of the equal-weight rule to correctly identify the coexistence chemical potential. To extract the infinite-volume value of ϕ_c from the finite-size data, it is, therefore, necessary to extrapolate to the thermodynamic limit. To this end, and in accordance with Eq. (3.6), we have plotted $\phi_{cx}(L)$, representing the first moment of the concentration distribution determined according to the equal weight criterion at the assigned value of ϵ_c, against $L^{(1-\alpha)/\nu}$. This extrapolation (Fig. 4) yields the infinite-volume estimate

$$\phi_c = 0.038\,13(19)$$

corresponding to a reduced A-monomer density $\phi_c/\phi_{\mathcal{N}} = 0.610(3)$. The finite-size shift in the value of $\phi_{cx}(L)$ is of order 2%.

We turn next to the determination of the field mixing parameters r and s. The value of r represents the limiting critical gradient of the coexistence curve which, to a good approximation, can be simply read off from Fig. 1 with the result $r = -0.97(3)$. Alternatively (and as detailed in [29]) r may be obtained as the gradient of the line tangent to the measured critical energy function [Eq. (2.11)] at $\phi = \phi_c$. Carrying out this procedure yields $r = -1.04(6)$.

The procedure for extracting the value of the field mixing parameter s from the concentration distribution is rather more involved, and has been described in detail elsewhere [29,30]. The basic strategy is to choose s such as to satisfy

$$\delta p_L(\phi) = -s \frac{\partial}{\partial \phi} \{ p_L(\phi) [\langle u(\phi) \rangle - u_c - r(\phi - \phi_c)] \} ,$$

where $\delta p_L(\phi)$ is the measured antisymmetric field mixing component of the critical concentration distribution [30],

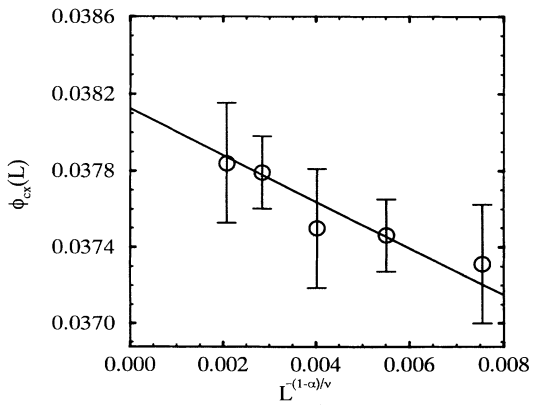

FIG. 4. Extrapolation of $\phi_{cx}(L)$, defined in the text, against $L^{-(1-\alpha)/\nu}$. The least squares fit yields an infinite volume estimate $\phi_c = 0.038\,23(19)$.

obtained by antisymmetrizing the concentration distribution about $\phi_c(L)$ and subtracting additional corrections associated with small departures from coexistence resulting from the failure of the equal weight rule. Carrying out this procedure for the $L=40$ and $L=64$ critical concentration distributions yields the field mixing components shown in Fig. 5. The associated estimate for s is 0.06(1). Also shown in Fig. 5 (solid line) is the predicted universal form of the 3D order parameter field mixing correction $-\partial/\partial x\ (\tilde{p}^{*}_{\mathcal{M}}(x)\tilde{\omega}^{*}(x))$ [cf., Eq. (2.10)] obtained from independent Ising model studies [37]. Clearly the measured functional form of the field mixing correction is in reasonable accord with the universal prediction. We attribute the residual discrepancies to field mixing contributions of order s^2 or higher, not included in Eq. (2.10). The directions of the two relevant scaling fields h and τ corresponding to the measured values of s and r are indicated in Fig. 1.

C. The critical limit revisited: Scaling operator distributions

In this subsection, we consider an alternative method for locating the critical point and determining the field mixing parameters s and r, which circumvents some of the difficulties associated with using the order parameter distribution alone.

The method focuses on the ordering and energylike scaling operator distributions $p_L(\mathcal{M})$ and $p_L(\mathcal{E})$ [cf., Eqs. (2.8a) and (2.8b)], which are obtained from the joint distribution of the energy density and concentration $p_L(\phi,u)$ as

$$p_L(\mathcal{M})=p_L\left[\frac{\phi-su}{1-sr}\right],\quad p_L(\mathcal{E})=p_L\left[\frac{u-r\phi}{1-sr}\right], \tag{3.8}$$

Precisely at criticality, $p_L(\mathcal{M})$ is expected to match the universal fixed point function $\tilde{p}^{*}_{\mathcal{M}}$. This suggests that the critical parameters can be readily located by simultaneously adjusting s, ϵ, and $\Delta\mu$ until $p_L\{[\phi-su]/(1-sr)\}$ matches $\tilde{p}^{*}_{\mathcal{M}}$ (modulo the choice of nonuniversal scale parameters implicit in the definition of the scaling variable). The results of performing this procedure for $p_L(\mathcal{M})$ are displayed in Fig. 6 for the $L=40$ and $L=64$ system sizes. The quality of the data collapse lends substantial support to the contention that the binary polymer critical point does indeed belong to the Ising universality class. The corresponding values of the critical parameters ϵ, $\Delta\mu_c$, and s are

$$\begin{aligned}\epsilon_c&=0.027\,56(15)\ ,\\ \Delta\mu_c&=0.003\,603(15)\ ,\\ s&=0.06(1)\ ,\end{aligned} \tag{3.9}$$

in good agreement with those determined previously. We note, however, that the present method permits the determination of s without the need to isolate the field mixing component of the concentration distribution, a procedure that is somewhat cumbersome and is only accurate to leading order in s [30].

The value of the field mixing parameter r, is intimately associated with the critical energy distribution $p_L(u)$, the form of which is shown in Fig. 7 for both the $L=40$ and $L=64$ system sizes. The corresponding mapping of the scaling operator distribution function $p_L\{[u-r\phi]/(1-sr)\}$ onto the universal energy distribution of the 3D Ising model, $\tilde{p}^{*}_{\mathcal{E}}$ is shown in Fig. 8. Again the agreement with the universal form is gratifying, although there are small discrepancies, which we attribute to corrections to scaling. The data collapse implies a value $r=-1.00(3)$,

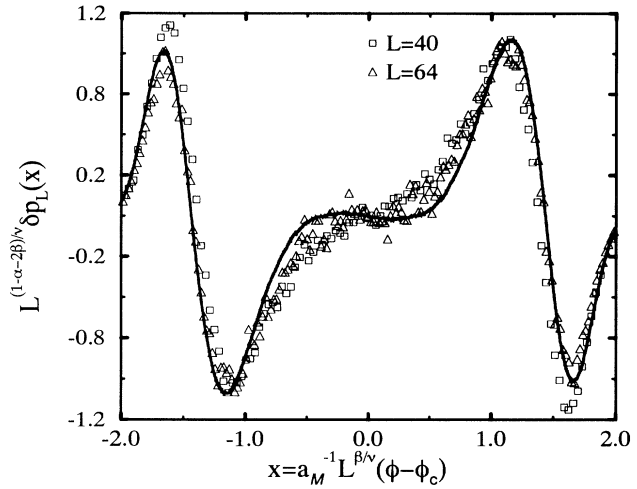

FIG. 5. The measured antisymmetric field mixing corrections $\delta p_L(x)$ of the $L=40$ and $L=64$ critical concentration distributions, expressed in terms of the scaling variable $x=a_{\mathcal{M}}^{-1}L^{\beta/\nu}(\phi-\phi_c)$ and shown as the data points. The data has itself been corrected for a small off-coexistence correction as described in the text. Also shown (full curve) is the universal prediction following from Eq. (2.10), utilizing predetermined Ising forms [37].

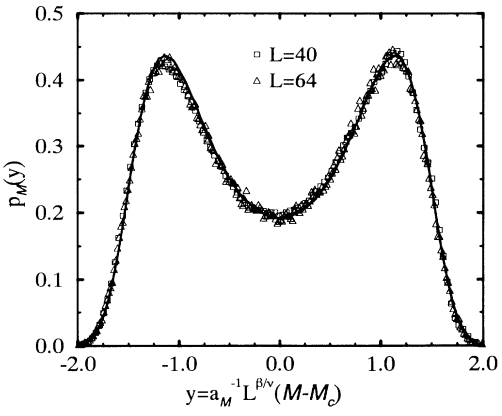

FIG. 6. The normalized distributions of the critical ordering operator $p_L(\mathcal{M})$ for the $L=40$ and $L=64$ system sizes, expressed as a function of the scaling variable $y=a_{\mathcal{M}}^{-1}L^{\beta/\nu}(\mathcal{M}-\mathcal{M}_c)$. The full curve is the fixed point function $\tilde{p}^{*}_{\mathcal{M}}$ appropriate to the Ising universality class [37]. The nonuniversal scale factor $a_{\mathcal{M}}^{-1}$ has been chosen so that the distributions have unit variance. The data collapse corresponds to a choice of the field mixing parameter $s=0.06(1)$. Statistical errors do not exceed the symbol sizes.

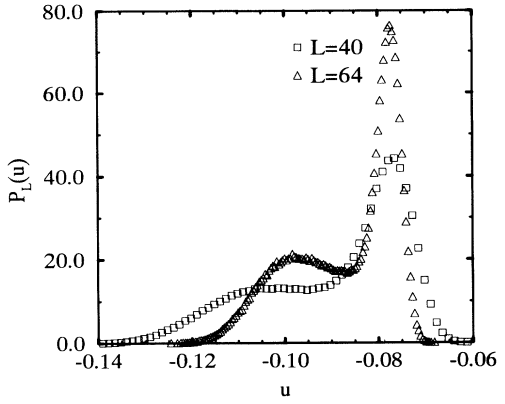

FIG. 7. The normalized distributions of the critical energy density $p_L(u)$ for the $L=40$ and $L=64$ system sizes.

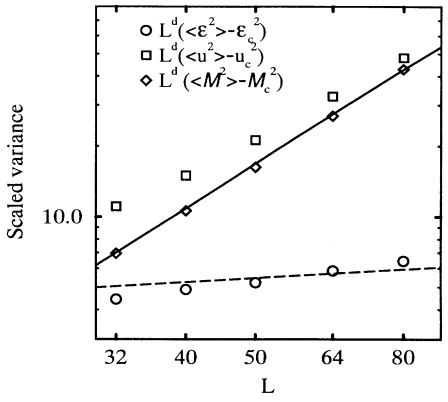

FIG. 9. The finite-size-scaling behavior of the variance of the critical energy, energy operator, and ordering operator distributions (cf., Figs. 7 and 8). The straight lines superimposed on the data points have the forms $0.0076L^{\gamma/\nu}$ (solid line) and $2.7L^{\alpha/\nu}$ (broken line), where $\gamma/\nu=1.970$, $\alpha/\nu=0.211$.

which also agrees to within error with the value obtained previously.

With regard to the critical energy distributions of Fig. 7, we note that the distributions are not at all reminiscent of the critical Ising energy distribution of Fig. 8. Neither, however, are they similar to $\tilde{p}^*_{\mathcal{M}}$ (cf., Fig. 6), which it was claimed they match in the limit $L\to\infty$ (cf., Sec. II). This discrepancy implies that the system size is still too small to reveal the asymptotic behavior; nevertheless, the data do afford a test of the *approach* to the limiting regime, via the FSS behavior of the variance of the energy distribution. Recalling Eq. (2.14), we anticipate that this variance exhibits the same FSS behavior as the Ising *susceptibility,* namely,

$$L^d(\langle u^2\rangle - u_c^2)\sim L^{\gamma/\nu}\ . \tag{3.10}$$

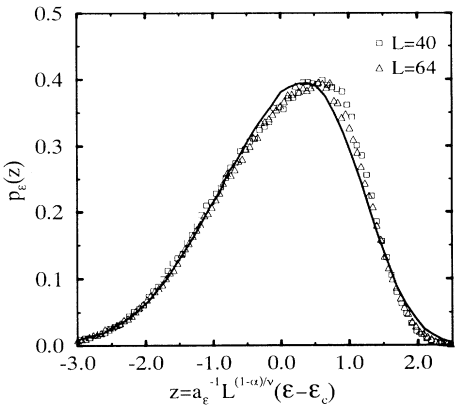

FIG. 8. The normalized distribution of the energylike operator $p_L(\mathcal{E})$ [cf., Eq. (2.8b)] expressed as a function of the scaling variable $z=a_{\mathcal{E}}^{-1}L^{(1-\alpha)/\nu}(\mathcal{E}-\mathcal{E}_c)$ for the $L=40$ and $L=64$ system sizes. The full curve is the fixed point function $\tilde{p}^*_{\mathcal{E}}$ appropriate to the Ising universality class [37]. The nonuniversal scale factor $a_{\mathcal{E}}^{-1}$, has been chosen so that the distributions have unit variance. The data collapse shown corresponds to a choice of the field mixing parameter $r=-1.00(3)$. Statistical errors do not exceed the symbol sizes.

By contrast, the variance of the scaling operator $\mathcal{E}$ is expected to display the FSS behavior of the Ising specific heat

$$L^d(\langle \mathcal{E}^2\rangle - \mathcal{E}_c^2)\sim L^{\alpha/\nu}\ . \tag{3.11}$$

Figure 9 shows the measured system size dependence of these two quantities at criticality. Also shown is the scaled variance of the ordering operator $L^d(\langle \mathcal{M}^2\rangle - \mathcal{M}_c^2)\sim L^{\gamma/\nu}$. Straight lines of the form $L^{\gamma/\nu}$ and $L^{\alpha/\nu}$ (indicative of the FSS behavior of the Ising susceptibility and specific heat, respectively) have also been superimposed on the data. Clearly, for large L, the scaling behavior of the variance of the energy distribution does indeed appear to approach that of the ordering operator distribution.

IV. MEAN-FIELD CALCULATIONS

In this section, we derive approximate formulas for the values of the field mixing parameters s and r on the basis of a mean-field calculation.

Within the well-known Flory-Huggins theory of polymer mixtures, the mean-field equation of state takes the form

$$\Delta\mu=\frac{1}{N_A}\ln(\rho)+\frac{1}{N_B}\ln(1-\rho)-2z\epsilon(2\rho-1)+C\ . \tag{4.1}$$

In this equation, $z\approx 2.7$ is the effective monomer coordination number, whose value we have obtained from the measured pair correlation function. $\rho=\phi/\phi_{\mathcal{N}}$ is the density of A-type monomers and the constant C is the entropy density difference of the pure phases, which is independent of temperature and composition. In what follows, we reexpress ρ by the concentration ϕ.

The critical point is defined by the condition

$$\frac{\partial}{\partial\phi}\Delta\mu_c=\frac{\partial^2}{\partial\phi^2}\Delta\mu_c=0\ , \tag{4.2}$$

where $\Delta\mu_c=\Delta\mu(\phi_c,\epsilon_c)$. This relation can be used to determine the critical concentration and critical well depth, for which one finds

$$\frac{\phi_c}{\phi_{\mathcal{N}}}=\frac{1}{1+1/\sqrt{k}} \quad \text{and} \quad \frac{1}{\epsilon_c}=z\frac{4N_AN_B}{(\sqrt{N_A}+\sqrt{N_B})^2} \tag{4.3}$$

Below the critical point, a first-order phase transition occurs between the A-rich and A-poor phases. To determine the location of the phase boundary, we employ a Landau expansion of the equation of state in terms of the small parameters $\delta\phi=\phi-\phi_c$ and $\delta\epsilon=\epsilon-\epsilon_c$:

$$\Delta\mu=\Delta\mu_c+r'\delta\epsilon-a\delta\epsilon\delta\phi+b\delta\phi^3+c\delta\phi^4+\cdots , \tag{4.4}$$

where the expansion coefficients take the form

$$\begin{aligned} r'&=-2z\left[2\frac{\phi_c}{\phi_{\mathcal{N}}}-1\right], \\ a&=\frac{4z}{\phi_{\mathcal{N}}}, \\ b&=\frac{(1+\sqrt{k})^4}{3\sqrt{k}N_A\phi_{\mathcal{N}}^3}, \\ c&=\frac{(k-1)(1+\sqrt{k})^4}{4kN_A\phi_{\mathcal{N}}^4}. \end{aligned} \tag{4.5}$$

The phase boundary itself is specified by the binodal condition

$$\Delta\mu_{\rm cx}(\epsilon)=\Delta\mu(\phi_+,\epsilon)=\Delta\mu(\phi_-,\epsilon)=\frac{\int_{\phi_-}^{\phi_+}d\phi\Delta\mu(\phi,\epsilon)}{\phi_+-\phi_-}, \tag{4.6}$$

where ϕ_- and ϕ_+ denote the concentration of A monomers in the A-poor phase and A-rich phases, respectively. Thus, to leading order in ϵ, the phase boundary is given by

$$\Delta\mu_{\rm cx}(\epsilon)=\Delta\mu_c+r'\delta\epsilon_c+\cdots . \tag{4.7}$$

Consequently, we can identify the expansion coefficient r' with the field mixing parameter r [cf., Eq. (2.5)] that controls the limiting critical gradient of the coexistence curve in the space of $\Delta\mu$ and ϵ. Substituting for $\Delta\mu_c$ and ϵ_c in Eq. (4.7) and setting $k=3$, we find $r=-1.45$, in order-of-magnitude agreement with the FSS analysis of the simulation data.

In order to calculate the value of the field mixing parameter s, it is necessary to obtain the concentration and energy densities of the coexisting phases near the critical point. The concentration of A-type monomers in each phase is given by

$$\delta\phi_\pm=\phi_\pm-\phi_c=\pm\left[\frac{a\delta\epsilon}{b}\right]^{1/2}-\frac{2ac\delta\epsilon}{5b^2}+\cdots , \tag{4.8}$$

so that the variation of the order parameter along the coexistence curve is

$$\langle\delta\phi\rangle=\left\{\frac{\phi_++\phi_-}{2}-\phi_c\right\}=-\frac{2ac\delta\epsilon}{5b^2} . \tag{4.9}$$

A similar calculation for the energy density yields

$$\begin{aligned} \langle u(\phi)\rangle&=-\frac{\phi_{\mathcal{N}}}{2}[z_s+z(2\rho-1)^2] \\ &=-\frac{\phi_{\mathcal{N}}}{2}\left[z_s+z\left[2\frac{\phi_c}{\phi_{\mathcal{N}}}-1\right]^2\right]+r\delta\phi-\frac{2z}{\phi_{\mathcal{N}}}\delta\phi^2 , \end{aligned} \tag{4.10}$$

where z_s is the coordination number of the intrachain thermal interactions. The variation of the energy density along the coexistence curve then follows as

$$\begin{aligned} \langle\delta u\rangle&=\frac{u(\phi_+)+u(\phi_-)}{2}-u(\phi_c) \\ &=-\frac{2za}{b\phi_{\mathcal{N}}}\left[1+r\frac{c\phi_{\mathcal{N}}}{5zb}\right]\delta\epsilon+\cdots . \end{aligned} \tag{4.11}$$

Now, since $(1-rs)\langle\mathcal{M}\rangle=\langle\delta\phi\rangle-s\langle\delta u\rangle$ vanishes along the coexistence line, Eqs. (4.9) and (4.11) yield the following

$$\begin{aligned} s=\frac{\langle\delta\phi\rangle}{\langle\delta u\rangle}&=\frac{c\phi_{\mathcal{N}}}{5zb(1+r\ c\phi_{\mathcal{N}}/5zb)} \\ &=\frac{3(k-1)}{20z\sqrt{k}\,[1+r\ 3(k-1)/20z\sqrt{k}\,]} . \end{aligned} \tag{4.12}$$

Thus, within the mean-field framework, the field mixing parameter s is controlled by the ratio of the fifth- and fourth-order coefficient of the Landau expansion of the free energy. For the present case ($k=3$) Eq. (4.12) yields $s=0.070$, in good agreement with the value obtained from the FSS analysis of the simulation data. It is also similar in magnitude to the values of s measured for the 2D Lennard-Jones fluid [29] and 2D asymmetric lattice gas model [30]. The sign of the product rs differs, however, from that found at the liquid-vapor critical point. In the present context this product is given by

$$\frac{rs}{1-rs}=-\frac{3}{10}\frac{(\sqrt{N_A}-\sqrt{N_B})^2}{\sqrt{N_AN_B}} . \tag{4.13}$$

However, an analogous treatment of the van der Waals fluid predicts a positive sign rs, in agreement with that found at the liquid-vapor critical point [29,30].

V. CONCLUDING REMARKS

In summary, we have employed a semi-grand-canonical Monte Carlo algorithm to explore the critical point behavior of a binary polymer mixture. The near-critical concentration and scaling operator distributions have been analyzed within the framework of a mixed-field finite-size scaling theory. The scaling operator distributions were found to match independently known universal forms, thereby confirming the essential Ising character of the binary polymer critical point. Interestingly, this universal behavior sets in on remarkably short length

scales, being already evident in systems of linear extent $L=32$, containing only an average of approximately 100 polymers.

Regarding the specific computational issues raised by our study, we find that the concentration distribution can be employed in conjunction with the cumulant intersection method and the equal weight rule to obtain a rather accurate estimate for the critical temperature and chemical potential. The accuracy of this estimate is not adversely affected by the antisymmetric (odd) field mixing contribution to the order parameter distribution, since only even moments of the distribution are featured in the cumulant ratio. Unfortunately, the method can lead to significant errors in estimates of the critical concentration ϕ_c, which *are* sensitive to the magnitude of the field mixing contribution. The infinite-volume value of ϕ_c must, therefore, be estimated by extrapolating the finite-size data to the thermodynamic limit (where the field mixing component vanishes). Estimates of the field mixing parameters s and r can also be extracted from the field mixing component of the order parameter distribution, although in practice we find that they can be determined more accurately and straightforwardly from the data collapse of the scaling operators onto their universal fixed point forms.

In addition to clarifying the universal aspects of the binary polymer critical point, the results of this study also serve more generally to underline the crucial role of field mixing in the behavior of critical fluids. This is exhibited most strikingly in the form of the critical energy distribution, which in contrast to models of the Ising symmetry, is doubly peaked with variance controlled by the Ising susceptibility exponent. Clearly, therefore, close attention must be paid to field mixing effects if one wishes to perform a comprehensive simulation study of critical fluids. In this regard, the scaling operator distributions are likely to prove themselves of considerable utility in future simulation studies. These operator distributions represent the natural extension to fluids of the order parameter distribution analysis deployed so successfully in critical phenomena studies of (Ising) magnetic systems. Provided, therefore, that one works within an ensemble that affords adequate sampling of the near-critical fluctuations, use of the operator distribution functions should also permit detailed studies of fluid critical behavior.

ACKNOWLEDGMENTS

The authors thank K. Binder for helpful discussions. N.B.W. acknowledges financial support from the Max Planck Institut für Polymerforschung, Mainz. Part of the simulations described here were performed on the KSR1 parallel computer at the Universität Mannheim and on the CRAY-YMP at the HLRZ Jülich. Partial support from the Deutsche Forschungsgemeinschaft (DFG) under Grant No. Bi314/3-2 is also gratefully acknowledged.

APPENDIX

In this appendix we give a brief description of our semi-grand-canonical algorithm for polymer mixtures with chain lengths $N_B=kN_A, k=3$. A more detailed presentation of the method can be found in Ref. [20].

As illustrated in Fig. 10 the SGCE Monte-Carlo moves consists in either joining together k A polymers to form a B chain, or alternatively, cutting a B polymer into k equal segments, each of which is then an A chain. The B chain formation step is attempted with probability $n_A/(n_A+n_B)$, and proceeds as follows. First one starts by choosing a random A-polymer end (a given end is selected with probability $1/2n_A$). One then determines the number ν_1 of neighboring A ends that satisfy the bonding constraints. Of the ν_1 possible ends to which a bond might be formed, one is chosen randomly and the ends connected together. In the same way one computes the number ν_2 of possible bonding partners for the remaining end of the second A polymer and makes a connection if possible. Thus, the proposition probability for B polymer formation is given by: $P^{\text{prop}}_{kA\to B'}=1/[2(n_A+n_B)\nu_1\nu_2]$. Finally, the move is accepted with probability

$$P^{\text{acc}}_{kA\to B'}=\min(1,\exp(-\beta\Delta E(kA\to B')-N_B\Delta\mu))$$

The formation procedure for A chains simply involves cutting a B chain into three equal parts, a procedure that

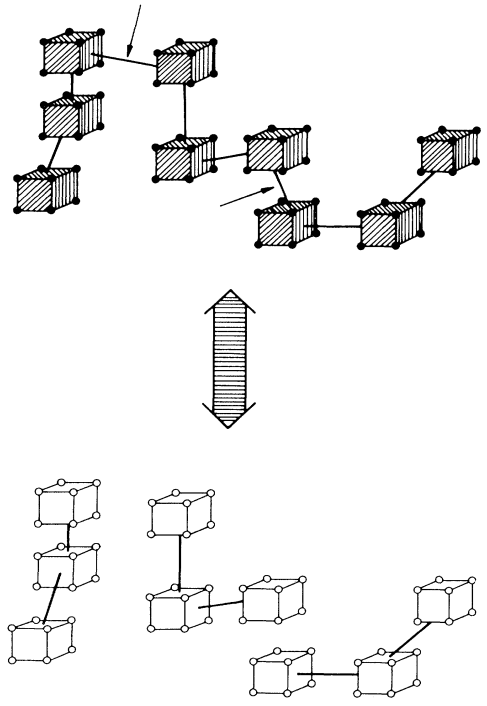

FIG. 10. Illustration of the semi-grand-canonical Monte Carlo moves for $k=3$ and $N_B=3$. Arrows indicate the bonds that are removed when one creates $k=3$ A chains or which have to be appropriately added in the inverse case. The monomer positions are left unaltered.

is attempted with probability $n_{B'}/(n_A+n_B)$. One end of a B chain is chosen with probability $1/2n_B$, and the cutting procedure starts from this end, leading to a proposition probability: $P^{\text{prop}}_{B'\to kA}=1/[2(n_A+n_B)]$. For the acceptance, one determines the possible number of bonding partners ν_1 and ν_2 for the corresponding inverse move and accepts the proposed move with probability

$$P^{\text{acc}}_{B'\to kA}=\frac{\min(1,\exp(-\beta\Delta E(B'\to kA)+N_B\Delta\mu))}{\nu_1\nu_2}\ .$$

Thus, the choice of the acceptance probabilities fulfills the detailed balance condition

$$P_{\text{eq}}(A)P^{\text{prop}}_{kA\to B'}P^{\text{acc}}_{kA\to B'}=P_{\text{eq}}(B')P^{\text{prop}}_{B'\to kA}P^{\text{acc}}_{B'\to kA}\ .$$

[1] A. Kumar, H. R. Krishnamurthy, and E. S. E. Gopal, Phys. Rep. **98**, 57 (1983).

[2] For a review, see, e.g., K. Binder, Adv. Polym. Sci. **112**, 181 (1994).

[3] N. Kuwahara, H. Sato, and K. Kubota, Phys. Rev. E **48**, 3176 (1993).

[4] F. S. Bates, J. H. Rosedale, P. Stepanek, T. P. Lodge, P. Wiltzius, G. H. Fredrickson, and R. O. Hjelm, Phys. Rev. Lett. **65**, 1893 (1990).

[5] S. Janssen, D. Schwahn, and T. Springer, Phys. Rev. Lett. **68**, 3180 (1992).

[6] D. W. Hair, E. K. Hobbie, A. I. Nakatani, and C. C. Han, J. Chem. Phys. **96**, 9133 (1992).

[7] N. Kuwahara, K. Hamano, and K. Kubota, Phys. Rev. A **44**, R6177 (1991).

[8] P. Stepanek, T. P. Lodge, C. Kedrowski, and F. S. Bates, J. Chem. Phys. **94**, 8289 (1991).

[9] D. Schwahn, K. Mortensen, T. Springer, H. Yee-Madeira, and R. Thomas, J. Chem. Phys. **87**, 6078 (1987).

[10] G. Meier, B. Momper, and E. W. Fischer, J. Chem. Phys. **97**, 5884 (1992).

[11] M. Lifschitz, J. Dudowicz, and K. F. Freed, J. Chem. Phys. **100**, 3957 (1994).

[12] V. L. Ginsburg, Fiz. Tverd. Tela (Leningrad) **2**, 2031 (1960) [Sov. Phys. Solid State **1**, 1824 (1960)]; P. G. de Gennes, J. Phys. Lett. (Paris) **38**, L-441 (1977); K. Binder, Phys. Rev. A **29**, 341 (1984).

[13] D. Schwahn, G. Meier, K. Mortensen, and S. Janssen, J. Phys. (Paris) II **4**, 837 (1994).

[14] K. Binder, in *Computational Modeling of Polymers*, edited by J. Bicerano (Marcel Dekker, New York, 1992), p. 221.

[15] W. Paul, K. Binder, D. W. Heermann, and K. Kremer, J. Phys. (Paris) II **1**, 37 (1991).

[16] A. Sariban and K. Binder, J. Chem. Phys. **86**, 5859 (1987).

[17] H.-P. Deutsch and K. Binder, Macromolecules **25**, 6214 (1992).

[18] H.-P. Deutsch, J. Chem. Phys. **99**, 4825 (1993).

[19] H.-P. Deutsch and K. Binder, J. Phys. (Paris) II **3**, 1049 (1993).

[20] M. Müller and K. Binder, Comput. Phys. Commun. **84**, 173 (1994); M. Müller (unpublished).

[21] J. J. Rehr and N. D. Mermin, Phys. Rev. A **8**, 472 (1973).

[22] J. V. Sengers and J. M. H. Levelt Sengers, Ann. Rev. Phys. Chem. **37**, 189 (1986).

[23] *Finite Size Scaling and Numerical Simulation of Statistical Systems*, edited by V. Privman (World Scientific, Singapore, 1990).

[24] A. D. Bruce, J. Phys. C **14**, 3667 (1981).

[25] K. Binder, Z. Phys. B **43**, 119 (1981).

[26] K. Binder and D. W. Heermann, *Monte-Carlo Simulations in Statistical Physics*, 2nd ed. (Springer, Heidelberg, 1992).

[27] D. Nicolaides and A. D. Bruce, J. Phys. A **21**, 233 (1988).

[28] A. D. Bruce and N. B. Wilding, Phys. Rev. Lett. **68**, 193 (1992).

[29] N. B. Wilding and A. D. Bruce, J. Phys. Condens. Matter **4**, 3087 (1992).

[30] N. B. Wilding, Z. Phys. B **93**, 119 (1993).

[31] D. Nakata, T. Dobashi, N. Kuwahara, and M. Kaneko, Phys. Rev. A **18**, 2683 (1978).

[32] I. Carmesin and K. Kremer, Macromolecules **21**, 2819 (1988); H. P. Deutsch and K. Binder, J. Chem. Phys. **94**, 2294 (1991).

[33] A. M. Ferrenberg and R. H. Swendsen, Phys. Rev. Lett. **61**, 2635 (1988); **63**, 1195 (1989); X. Bennett, J. Comp. Phys. **22**, 245 (1979).

[34] H.-P. Deutsch, J. Stat. Phys. **67**, 1039 (1992).

[35] C. Borgs and R. Kotecky, J. Stat. Phys. **60**, 79 (1990); Phys. Rev. Lett. **68**, 1734 (1992); C. Borgs and S. Kappler, Phys. Lett. A **171**, 37 (1992).

[36] A. M. Ferrenberg and D. P. Landau, Phys. Rev. B **44**, 5081 (1991).

[37] R. Hilfer and N. B. Wilding (unpublished).